Low-lying states of the ^{132}Ba nucleus within the nucleon-pair approximation

Y. Y. Cheng,[1] Y. Lei,[2] Y. M. Zhao,[1,3,*] and A. Arima[1,4]

[1]*Department of Physics and Astronomy, Shanghai Jiao Tong University, Shanghai 200240, China*
[2]*Key Laboratory of Neutron Physics, Institute of Nuclear Physics and Chemistry, China Academy of Engineering Physics,
Mianyang 621900, China*
[3]*IFSA Collaborative Innovation Center, Shanghai Jiao Tong University, Shanghai 200240, China*
[4]*Musashi Gakuen, 1-26-1 Toyotamakami Nerima-ku, Tokyo 176-8533, Japan*

In this paper we study the low-lying states of the ^{132}Ba nucleus within the nucleon-pair approximation, with our focus on the mechanism of band-crossing in the yrast band and two side bands headed by the 5_1^- and 6_1^- states, respectively. Two mechanisms of the back-bending phenomenon in the yrast band previously suggested, i.e., the contribution of noncollective pairs with two $h_{11/2}$ neutron holes coupled to various spins (called H pairs for short) and the coupling of two neutron pairs with negative parity, are reconciled on the same footing and are found to be complementary in the description of low-lying states of the ^{132}Ba nucleus. This is carried out by nucleon-pair-approximation calculation in the proton configuration space constructed by collective SD pairs, coupled with the neutron configuration space constructed by SD pairs, H pairs, and collective negative-parity pairs of spin from 4 to 7. Our calculations show that back-bending exists in the 13_1^- state in the band based on the 5_1^- state, and in the 14_1^- state in the band based on the 6_1^- state, in addition to the back-bending in the 10_1^+ state in the yrast band. These back-bendings are interpreted in terms of the $(\nu h_{11/2})^{-2}$ alignment. We also perform calculations in a number of selected subspaces for neutron configuration. We show that the states above the corresponding back-bendings are reasonably represented by the negative-parity neutron pairs and better represented by the spin-10 H pair. In order to reproduce the experimental value of $B(E2,10_1^+ \rightarrow 8_1^+)$, the configurations of negative-parity neutron pairs are essential.

PACS number(s): 21.10.Re, 21.60.Ev, 23.20.Js, 27.60.+j

I. INTRODUCTION

Xe, Ba, and Ce nuclei in the $A \sim 130$ mass region are transitional nuclei exhibiting γ softness. The low-lying collective states as well as the back-bending phenomena at higher spins in these nuclei have attracted much attention. Theoretically, the low-lying collective states, in particular the quasi-γ bands of these nuclei, were suggested to be well described by O(6) symmetry in the framework of the interacting boson model [1,2], and by SO(6) symmetry in the framework of the fermion dynamical symmetry model [3]. The truncated scheme of the shell model constructed of SD nucleon pairs also provides a good description of the low-lying collective states in this region [4–6].

The structure of ^{132}Ba has also been studied in many experimental measurements [7–14]. The back-bending of the yrast band in the 10_1^+ state leads to an irregularity of level energy for the 10_1^+ state and the very small value of $B(E2,10_1^+ \rightarrow 8_1^+)$ [7]. The experimental value of the g factor [10,11] further indicates that this back-bending is given by the alignment of two $h_{11/2}$ neutron holes rather than $h_{11/2}$ protons. For negative-parity bands of ^{132}Ba, two bands built on the 5_1^- and 6_1^- states were suggested to be based on the two-quasineutron configuration, and the back-bendings in these two bands were suggested to be also caused by the alignment of $h_{11/2}$ neutron holes [8,9].

To describe back-bending phenomena, theoretical studies were performed in an extended interacting boson model with

the model space constructed of one nucleon pair coupled to sd bosons [15–17]. In Ref. [18], nucleon-pair bases constructed of noncollective spin-0, -2, -4, -6, -8, and -10 pairs formed by two $h_{11/2}$ neutron holes, denoted as H pairs, coupled to traditional SD nucleon pairs, were considered in order to describe the alignment of two $h_{11/2}$ neutron holes in the yrast band of ^{132}Ba. In the configuration space constructed using such nucleon pairs, a good description of the back-bending phenomena of the yrast bands in the neighboring ^{132,134,136}Ce was also achieved [19]. Yet the adopted interaction parameters for low-lying states below the back-bending in terms of SD nucleon pairs are quite different from those for low-lying states including the back-bending in terms of the $SD + H$ pairs [18].

Very recently, another picture, i.e., coupling of two neutron pairs with negative parity, was suggested as a surrogate for the alignment of two $h_{11/2}$ neutron holes [20]. In Ref. [21], negative-parity nucleon pairs were introduced to describe negative-parity states of even-even nuclei. Interestingly, it was shown in Ref. [20] that the alignment of two $h_{11/2}$ neutron holes and the corresponding back-bending phenomena in both the yrast band and the two side bands headed by the 5_1^- and 6_1^- states of the ^{132}Ba nucleus were well described in terms of two negative-parity neutron pairs. It was also pointed out in Ref. [20] that, as the contribution from two neutron holes in the $d_{3/2}$ and/or $s_{1/2}$ orbits is small in the large total spin coupled by two negative-parity pairs, this large total spin is mainly given by the alignment of two $h_{11/2}$ neutron holes.

In this paper we study low-lying states of the ^{132}Ba nucleus within the nucleon-pair approximation (NPA), with our focus

---

*Corresponding author: ymzhao@sjtu.edu.cn

on the mechanism of band-crossing in the yrast band and two side bands headed by the 5_1^- and 6_1^- states. We reconcile the two pictures suggested in Refs. [18] and [20] by the NPA calculation in a large neutron-pair configuration space for which the building blocks include traditional SD pairs, H pairs, and collective negative-parity pairs of spin from 4 to 7. We show that these two pictures are complementary in achieving a good description of the low-lying states in this nucleus.

This paper is organized as follows. In Sec. II we give a brief introduction to the NPA, in Sec. III we present the calculated results obtained in the above configuration space, in comparison with theoretical results based on a number of selected subspaces, and in Sec. IV we summarize and conclude this paper.

II. THE NUCLEON-PAIR APPROXIMATION OF THE SHELL MODEL

The NPA is an efficient truncation scheme of the gigantic shell model space. If all possible nucleon pairs are considered, the NPA results coincide with those of the full shell model calculation; if only a few important nucleon pairs are considered, the NPA model space is tremendously smaller than the exact shell-model space. The general framework of the NPA was proposed by Chen in Ref. [22] and refined in Ref. [23]. For a comprehensive review, see Ref. [24].

A. Nucleon-pair basis

In the NPA, one can assume both noncollective pairs and collective pairs in constructing the model space. Supposing $C_a^\dagger$ ($C_b^\dagger$) is a creation operator for a nucleon in the a (b) orbit, we denote

$$A^{r\dagger}(ab) = (C_a^\dagger \times C_b^\dagger)^r, \quad A^{r\dagger} = \sum_{ab} y(abr)A^{r\dagger}(ab). \quad (1)$$

Here r is the spin of the nucleon pair. $A^{r\dagger}(ab)$ is called the creation operator of a noncollective pair with one nucleon in the a orbit and the other in the b orbit. $A^{r\dagger}$ is called a collective pair with spin r, and $y(abr)$ is called the structure coefficient.

The configuration space of the NPA is constructed using nucleon pairs defined above. For a system with $2N$ identical nucleons, the basis is constructed by coupling N nucleon pairs successively:

$$|\alpha J_N\rangle = ((A^{r_1\dagger} \times A^{r_2\dagger})^{(J_2)} \times \cdots \times A^{r_N\dagger})^{(J_N)}|0\rangle. \quad (2)$$

If valence neutrons and protons do not belong to the same shell, or the neutron number of a given nucleus is considerably larger than its proton number, as is the case in this paper, the proton-neutron configuration space is constructed as $(|\alpha_\pi J_\pi\rangle \otimes |\alpha_\nu J_\nu\rangle)^J$. If the proton and neutron numbers are very close to each other, and valence protons and neutrons fill in the same orbit(s), one should construct the nucleon-pair basis with a given spin and isospin, as demonstrated in Refs. [24] and [25].

The structure coefficients of collective pairs are determined in the following procedures. Given the interaction parameters of the neutron Hamiltonian H_ν (defined in the next subsection),

we diagonalize H_ν in the subspace constructed by all possible noncollective spin-0 neutron pairs, denoted as S_j. By maximizing the overlap between the ground state so obtained and the basis constructed of the collective spin-0 neutron pair, denoted as S, we obtain the structure coefficients $y(jj0)$. The structure coefficients of collective non-S pairs are obtained as follows: we diagonalize the Hamiltonian in the $(S^\dagger)^{(N-1)}A^{r\dagger}(j_1 j_2)$ [$S^\dagger$ is the collective pair with spin 0 and $A^{r\dagger}(j_1 j_2)$ is the noncollective pair with spin $r \neq 0$] space, with j_1, j_2 running over all the single-particle orbits. The lowest-state wave function is written as $(S^\dagger)^{(N-1)}\sum_{j_1 j_2} c(j_1 j_2)A^{r\dagger}(j_1 j_2)$, and we assume $y(j_1 j_2 r) = c(j_1 j_2)$. The structure coefficients of collective proton pairs are determined in the same way.

B. Shell model Hamiltonian and electromagnetic multipole operator

In this work we adopt the phenomenological Hamiltonian, which includes the single-particle energy, monopole pairing, quadrupole pairing, and quadrupole-quadrupole interaction. The form of our Hamiltonian is

$$H = \sum_{\sigma=\pi,\nu} H_\sigma + H_{\pi\nu},$$

$$H_\sigma = \sum_{j_\sigma} \varepsilon_{j_\sigma} \hat{n}_{j_\sigma} + \sum_{s=0,2} G_\sigma^s \mathcal{P}_\sigma^{s\dagger} \cdot \tilde{\mathcal{P}}_\sigma^s + \kappa_\sigma Q_\sigma \cdot Q_\sigma,$$

$$H_{\pi\nu} = \kappa_{\pi\nu} Q_\pi \cdot Q_\nu, \quad (3)$$

where ε_{j_σ} is the single-particle energy; G_σ^0, G_σ^2, and κ_σ are the strength parameters of the monopole pairing, quadrupole pairing, and quadrupole-quadrupole interaction between like nucleons; and $\kappa_{\pi\nu}$ is the strength parameter of the proton-neutron quadrupole-quadrupole interaction. The operators in Eq. (3) are defined as

$$\mathcal{P}^{0\dagger} = \sum_j \frac{\sqrt{2j+1}}{2}(C_j^+ \times C_j^+)^{(0)},$$

$$\mathcal{P}^{2\dagger} = \sum_{jj'} q(jj'2)(C_j^+ \times C_{j'}^+)^{(2)},$$

$$\tilde{\mathcal{P}}^0 = -\sum_j \frac{\sqrt{2j+1}}{2}(\tilde{C}_j \times \tilde{C}_j)^{(0)},$$

$$\tilde{\mathcal{P}}^2 = -\sum_{jj'} q(jj'2)(\tilde{C}_j \times \tilde{C}_{j'})^{(2)},$$

$$Q = \sum_{jj'} q(jj'2)(C_j^+ \times \tilde{C}_{j'})^{(2)},$$

$$q(jj'2) = \frac{(j\|r^2Y^2\|j')}{\sqrt{5}r_0^2}. \quad (4)$$

Here r_0 is the oscillator parameter, and $r_0^2 = 1.012A^{1/3}$ fm^2. The definition of the reduced matrix elements can be found in Eq. (8.4) in Ref. [26].

For the ^{132}Ba nucleus, both the particle-like valence protons and the hole-like valence neutrons occupy the orbits of the 50-82 major shell. The single-particle energies of the proton $d_{3/2}$, $d_{5/2}$, $g_{7/2}$, and $h_{11/2}$ orbits are based on the single-particle

TABLE I. Hamiltonian parameters (in MeV) adopted in this work. Single-particle energies of proton orbits with respect to $\pi g_{7/2}$ and single-hole energies of neutron orbits with respect to $\nu d_{3/2}$ are taken from Refs. [20,27]. Parameters for monopole pairing, quadrupole pairing, and quadrupole-quadrupole interaction are adjusted to fit the experimental data of level spectra. As the proton-neutron quadrupole-quadrupole interaction is between particle-like valence protons and hole-like valence neutrons in this work, the strength parameter $\kappa_{\pi\nu}$ is positive.

	$s_{1/2}$	$d_{3/2}$	$d_{5/2}$	$g_{7/2}$	$h_{11/2}$
ε_π	2.990	2.440	0.962	0.000	2.792
ε_ν	0.332	0.000	1.655	2.434	0.242
G_π^0	G_π^2	κ_π	G_ν^0	G_ν^2	κ_ν	$\kappa_{\pi\nu}$
-0.150	-0.035	-0.040	-0.180	-0.035	-0.065	0.070

states of ^{133}Sb [27], and the single-hole energies of the neutron $s_{1/2}$, $d_{3/2}$, $d_{5/2}$, and $g_{7/2}$ orbits are based on the single-hole states of ^{131}Sn [27]. The single-particle energy of $\pi s_{1/2}$ and the single-hole energy of $\nu h_{11/2}$ are not yet available, and their values adopted in this paper are taken from Ref. [20]. The strength parameters of the monopole pairing, quadrupole pairing, and quadrupole-quadrupole interaction are adjusted to fit the experimental data of level spectra. As valence protons are particle-like and valence neutrons are hole-like, the strength parameter of the proton-neutron quadrupole-quadrupole interaction is positive. In Table I we list all the Hamiltonian parameters adopted in this work.

The electric quadrupole operator is defined as

$$T(E2) = e_\pi Q_\pi + e_\nu Q_\nu, \qquad (5)$$

where the operator Q is defined in Eq. (4). The reduced electric quadrupole transition probability is given by

$$B(E2) = \frac{1}{2J_i + 1}(\alpha_f J_f \| T(E2) \| \alpha_i J_i)^2. \qquad (6)$$

The magnetic dipole operator is defined as

$$T(M1) = g_{l\pi} L_\pi + g_{s\pi} S_\pi + g_{l\nu} L_\nu + g_{s\nu} S_\nu. \qquad (7)$$

The magnetic dipole moment is given by the diagonal matrix element of $T(M1)$,

$$\mu = \sqrt{\frac{4\pi}{3}} \langle JM = J | T(M1) | JM = J \rangle, \qquad (8)$$

and the reduced magnetic dipole transition probability is given by

$$B(M1) = \frac{1}{2J_i + 1}(\alpha_f J_f \| T(M1) \| \alpha_i J_i)^2. \qquad (9)$$

The one-body operators L and S in Eq. (7) are defined as

$$L = \sum_{jj'} q_l(jj'1)(C_j^+ \times \tilde{C}_{j'})^{(1)},$$

$$S = \sum_{jj'} q_s(jj'1)(C_j^+ \times \tilde{C}_{j'})^{(1)},$$

$$q_l(jj'1) = \delta_{ll'}(-1)^{l+1/2+j'}\sqrt{\frac{l(l+1)}{3}}\hat{j}\hat{j}'\hat{l}\begin{Bmatrix} j & j' & 1 \\ l' & l & \frac{1}{2} \end{Bmatrix},$$

$$q_s(jj'1) = \delta_{ll'}(-1)^{l+1/2+j}\frac{1}{\sqrt{2}}\hat{j}\hat{j}'\begin{Bmatrix} j & j' & 1 \\ \frac{1}{2} & \frac{1}{2} & l \end{Bmatrix}. \qquad (10)$$

In this paper the effective charge, orbital gyromagnetic ratio, and spin gyromagnetic ratio of valence nucleons are adopted as follows: $e_\pi = 2e$, $e_\nu = -e$; $g_{\pi l} = 0.90\mu_N$, $g_{\nu l} = 0.05\mu_N$; and $g_{\pi s} = 5.586 \times 0.7\mu_N$, $g_{\nu s} = -3.826 \times 0.7\mu_N$.

III. RESULTS AND DISCUSSION

In this paper the proton configuration space is constructed of the collective positive-parity spin-0 and spin-2 pairs, denoted as S and D. The neutron configuration space has five options, and we perform calculations using all of them, denoted as Cal-1 to Cal-5, respectively. In all calculations, the Hamiltonian parameters are kept *unchanged*, as listed in Table I. The building blocks of these five neutron configuration spaces are as follows.

Cal-1: Collective SD pairs; noncollective pairs consisting of two $h_{11/2}$ neutron holes coupled to spin 0, 2, 4, 6, 8, and 10, denoted as $H^{(0)}$, $H^{(2)}$, ..., $H^{(10)}$; and collective negative-parity pairs of spin 4, 5, 6, and 7, denoted as $\mathcal{G}$, $\mathcal{H}$, $\mathcal{I}$, and $\mathcal{J}$, respectively.

Cal-2: Collective SD pairs and negative-parity $\mathcal{G}$, $\mathcal{H}$, $\mathcal{I}$, and $\mathcal{J}$ pairs (similar to the neutron configurations in Ref. [20]).

Cal-3: Collective SD pairs and $H^{(0)}$, $H^{(2)}$, ..., $H^{(10)}$ pairs for positive-parity states (similar to the neutron configurations in Ref. [18]). In order to describe negative-parity states in Cal-3, one of the above $\mathcal{G}$, $\mathcal{H}$, $\mathcal{I}$, and $\mathcal{J}$ pairs is included in each pair basis for negative-parity states.

Cal-4: Same as Cal-3 except that H pairs are restricted to the $H^{(10)}$ pair only.

Cal-5: Same as Cal-4 except the $H^{(10)}$ pair is excluded.

The neutron configuration space in Cal-1 is the largest, and all other spaces (Cal-2 to Cal-5) are subspaces of that in Cal-1. From Table I one expects that neutron holes predominantly occupy the three lowest orbits, $s_{1/2}$, $d_{3/2}$ and $h_{11/2}$, and the possible spin of two neutron holes in these orbits coupled to a negative-parity pair is from 4 to 7. Therefore neutron pairs with negative parity and spin from 4 to 7, which are considered in this work, are more important than other negative-parity neutron pairs in low-lying states. We should note that in Cal-3 to Cal-5, there is no contribution from negative-parity pairs in positive-parity states, as the number of negative pairs is limited to one therein.

In this paper we study four low-lying bands of the ^{132}Ba nucleus, i.e., the yrast band, quasi-γ band, and two negative-parity bands with the bandheads of the 5_1^- and 6_1^- states. We plot the experimental level spectra in Fig. 1(a) and our calculated results for these bands in Figs. 1(b)–1(f), corresponding to Cal-1 to Cal-5, respectively. In each panel
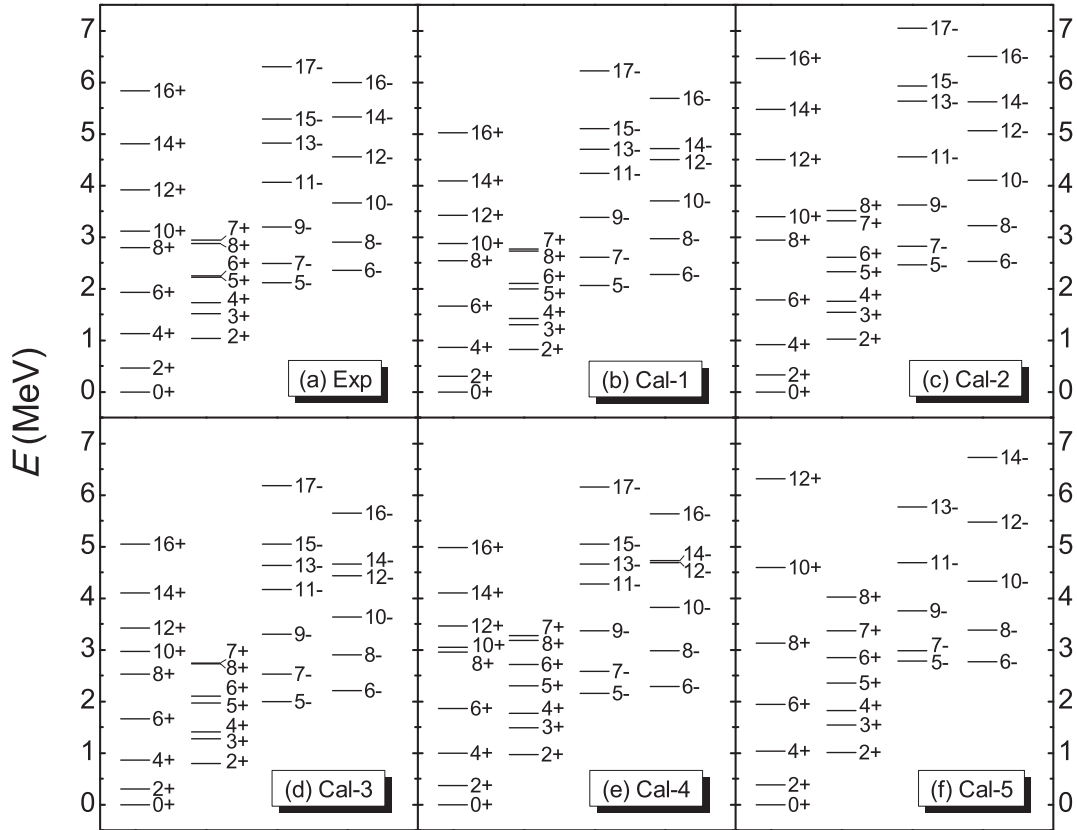
FIG. 1. Level spectra of the ^{132}Ba nucleus. (a) Experimental results taken from Ref. [27]; (b–f) Calculated results obtained in five nucleon-pair configuration spaces, denoted as Cal-1 to Cal-5, respectively. In all these calculations, proton configurations are constructed of SD pairs. In Cal-1, the building blocks of neutron configurations include SD pairs, the noncollective pairs with two $h_{11/2}$ neutron holes (called H pairs) coupled to spin 0, 2, 4, 6, 8, and 10, denoted as $H^{(0)}$, $H^{(2)}$,...,$H^{(10)}$, and the collective negative-parity pairs of spin 4, 5, 6, and 7, denoted as $\mathcal{G}$, $\mathcal{H}$, $\mathcal{I}$, and $\mathcal{J}$. This is the largest configuration space here; the configuration spaces in Cal-2 to Cal-5 are subspaces of that in Cal-1. In Cal-2, the building blocks of neutron configurations include SD pairs and negative-parity pairs ($\mathcal{G}$, $\mathcal{H}$, $\mathcal{I}$, and $\mathcal{J}$). In Cal-3, the positive-parity configuration basis for neutrons is constructed of SD pairs and H pairs, and the negative-parity configuration basis, of SDH pairs coupled to one of the four negative-parity pairs. In Cal-4, the building blocks are the same as those in Cal-3, except that H pairs are restricted to $H^{(10)}$. In Cal-5, the building blocks are the same as those in Cal-4 except that the $H^{(10)}$ pair is excluded.

the four bands are presented from left to right. In Fig. 2 we show the evolution of $B(E2, I \rightarrow I-2)$ values and g factors versus the spin of the state given by Cal-1 to Cal-4, respectively, for the yrast band [Figs. 2(a) and 2(d)], the band based on the 5_1^- state [Figs. 2(b) and 2(e)], and the band based on the 6_1^- state [Figs. 2(c) and 2(f)], in comparison with available experimental data. In Fig. 3 we present the overlaps of wave functions calculated in Cal-2 to Cal 5 with those in Cal-1. The model space in Cal-1 is the largest for all NPA calculations hitherto; we therefore tabulate numerical results of Cal-1. In Table II we present the $B(E2, I \rightarrow I-2)$ values and g factors for the yrast band and two negative-parity bands, in Table III we present the $B(E2)$ and $B(M1)$ values of the interband transitions between the two negative-parity bands, and in Table IV we present the relative $B(E2)$ values for the intraband transitions of the quasi-γ band and the interband transitions from the quasi-γ band to the yrast band, as well as their comparison with experimental data. One sees that the energy spectra, $B(E2)$ values, and g factors obtained in Cal-1 agree well with the experimental data.

Let us first discuss the yrast band. For states below 10_1^+, a regular level structure is observed experimentally, with a relatively large value of $B(E2, 2_1^+ \rightarrow 0_1^+)$. In Fig. 3(a), one sees the overlaps between the wave functions of the 0_1^+, 2_1^+, 4_1^+, and 6_1^+ states calculated in the simple SD-pair subspace (namely, Cal-5) and those in Cal-1 are quite large (>0.8). This means that the SD-pair approximation gives a rather good description of these states. Correspondingly, in Fig. 1 one sees that the level spacings between the 0_1^+, 2_1^+, 4_1^+, and 6_1^+ states obtained in Cal-1 to Cal-5 are close to each other and are consistent with the experimental results. For the 8_1^+ state, the overlap between the wave function in Cal-1 and that in Cal-5 is only ~ 0.5, and the overlap between Cal-1 and Cal-2 is close to that between Cal-1 and Cal-5, which means that the contribution of negative-parity neutron pairs is small in the 8_1^+ state. On the other hand, the overlap between the wave function in Cal-1 and that in Cal-3 is very close to 1, which means that the contribution from the H pairs is important. One also sees in Fig. 3(a) that the overlap between the wave function in Cal-3 and that in Cal-4 is ~ 0.7 for the 8_1^+ state, which means that the configuration of the $H^{(10)}$
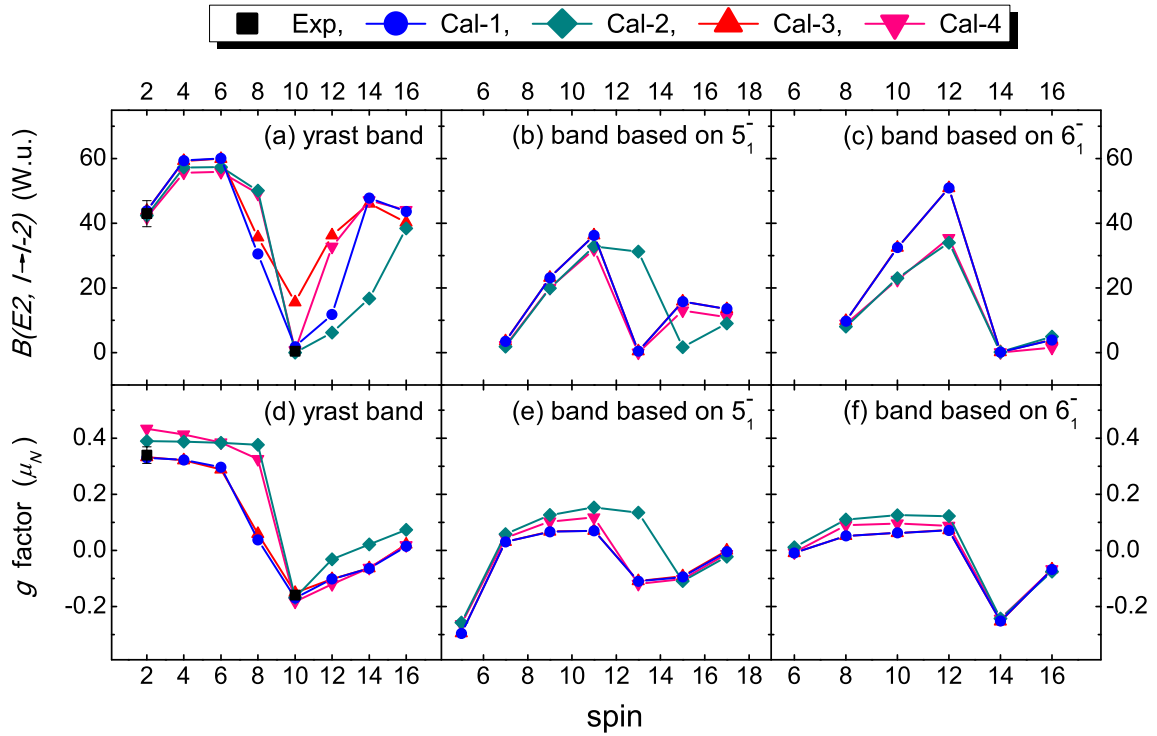
FIG. 2. (Color online) (a–c) $B(E2, I \rightarrow I - 2)$ values (in W.u.) and (d–f) g factors (in μ_N) versus the spin of the state. (a, d) yrast band; (b, e) band based on the 5_1^- state; (c, f) band based on the 6_1^- state. Experimental data [filled (black) squares] are taken from Ref. [27]; calculated results are obtained in the configuration spaces of Cal-1 [filled (blue) circles], Cal-2 [filled (green) diamonds], Cal-3 [filled upward (red) triangles], and Cal-4 [filled downward (pink) triangles], respectively.

pair is not very important. A numerical experiment on further inclusion of the $H^{(8)}$ pair in Cal-4 yields a wave function overlapping very well with that in Cal-3 (~ 0.9). Therefore, the $H^{(8)}$ pair is essential in the 8_1^+ state.

For the yrast band, an anomalously small spacing between the 10_1^+ and 8_1^+ states and a very small value of $B(E2, 10_1^+ \rightarrow 8_1^+)$ were observed in experiments, suggesting a back-bending phenomenon in the 10_1^+ state. The measured g factor of the 10_1^+ state further suggested the alignment picture of two $h_{11/2}$ neutron holes, denoted as $(\nu h_{11/2})^{-2}$. In Figs. 1 and 2, one sees that these features of the back-bending phenomenon in the yrast band are well reproduced in Cal-1. In Fig. 3(a) one sees that the overlaps between the wave functions of the 10_1^+ and 12_1^+ states in Cal-1 and those in Cal-5 are close to 0. Indeed this is expected, because the $(\nu h_{11/2})^{-2}$ alignment is excluded in the neutron subspace of Cal-5. For the 10_1^+ state, both the overlap between the wave function in Cal-1 and that in Cal-2 and the overlap between the wave function in Cal-1 and that in Cal-3 are around 0.85. This means that the subspace of Cal-2 and that of Cal-3 are comparably good for this state. Yet the overlap between the wave function of the 10_1^+ state in Cal-2 and that in Cal-3 is < 0.6, which means that the two pictures, one of which is represented by the coupling of two negative-parity neutron pairs and the other of which is represented by H pairs, are relevant and complementary in obtaining a good description of the 10_1^+ state. In Fig. 2 one sees that the $B(E2, 10_1^+ \rightarrow 8_1^+)$ of Cal-3 is considerably larger than the experimental data, while the

$B(E2, 10_1^+ \rightarrow 8_1^+)$ of Cal-2 agrees well with the experimental data, which means that the contribution of configurations from negative-parity nucleon pairs cannot be ignored in order to reproduce well the experimental value of $B(E2, 10_1^+ \rightarrow 8_1^+)$. It is worthwhile to mention, although our interaction parameters are different from those used in Refs. [18] and [20], the calculated $B(E2, 10_1^+ \rightarrow 8_1^+)$ in Cal-3 is close to that in Ref. [18] (~ 15 W.u.), and the $B(E2, 10_1^+ \rightarrow 8_1^+)$ in Cal-2 is close to that in Ref. [20]. This suggests that the above conclusion is robust with respect to the interaction parameters.

As for the states of the yrast band above the 10_1^+ state, one sees in Fig. 3(a) that the overlaps between the wave functions in Cal-1 and those in Cal-3 are very close to 1, while the overlaps between the wave functions in Cal-1 and those in Cal-2 are considerably smaller. This is consistent with the results in Fig. 1, where the energies of the 12_1^+, 14_1^+, and 16_1^+ states in Cal-2 are considerably higher than those obtained in Cal-3. The overlaps between the wave functions in Cal-1 and those in Cal-2 for these states are very close to the corresponding overlaps between wave functions in Cal-2 and those in Cal-3. These results demonstrate that for these states the $(\nu h_{11/2})^{-2}$ alignment can be described well by H pairs. In Fig. 3(a) one also sees that the overlaps between the wave functions of the 12_1^+, 14_1^+, and 16_1^+ states obtained in Cal-3 and those in Cal-4 are close to 1, which shows that a good description of these states is obtained by using the simple SD pairs coupled with the $H^{(10)}$ pair.

We note that the theoretical excited energies of the 12_1^+, 14_1^+, and 16_1^+ states (i.e., after the back-bending) in Cal-1
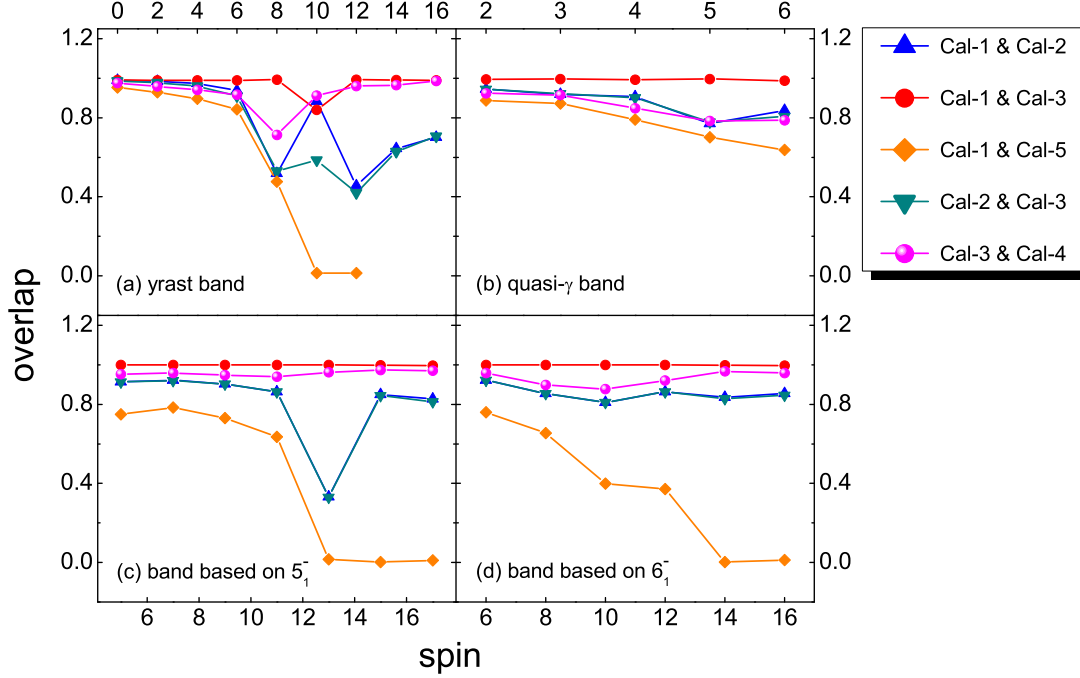
FIG. 3. (Color online) Overlaps of wave functions in the five sets of calculations (Cal-1 to Cal-5) versus the spin of the state. (a) yrast band, (b) quasi-γ band, (c) band based on 5_1^-, and (d) band based on 6_1^-. Overlaps between the wave functions in Cal-1 and those in Cal-2 are labeled as Cal-1 & Cal-2, overlaps between wave functions in Cal-1 and Cal-3 are labeled as Cal-1 & Cal-3, and so on.

are systematically smaller than the experimental values. This underestimation might be originated from the form of our simple Hamiltonian. As in the low-lying states of the ^{132}Ba nucleus valence protons predominantly occupy the $g_{7/2}$ and $d_{5/2}$ orbits, the octupole-octupole proton-neutron interaction between particle-like $g_{7/2}/d_{5/2}$ protons and hole-like $h_{11/2}$ neutrons, not considered in this work, might play an important role in these states above the back-bending.

We now turn to the quasi-γ band, which consists of the second excited states with positive parity and even spins, as well as the first excited states with positive parity and odd spins. In Fig. 1 one sees that the level spectra of the quasi-γ band obtained in Cal-1 agree well with the experimental data. In Table IV one sees that the experimental relative $B(E2)$ values for the intraband transitions of the quasi-γ band and the interband transitions from the quasi-γ band to the yrast band are reasonably reproduced in Cal-1. In Fig. 3(b), the overlaps between the wave functions of the quasi-γ band obtained in Cal-1 and those in Cal-3 are very close to 1. The SD-pair approximation, namely, Cal-5, gives a good description of the states of the quasi-γ band with lower spins. As the spin of the state increases, one sees that the overlaps between Cal-1 and Cal-5 decrease. This means that the contribution from the H pairs becomes more and more important as the spin increases in the quasi-γ band.

Finally, we come to the two negative-parity bands with the bandheads of the 5_1^- and 6_1^- states. These two bands were suggested to be based on the two-quasineutron configuration [8,9]. We note that a few states in these two bands are not the yrast states with negative parity, and some states with the same spin and parity in the other two bands headed by

the 7^- and 8^- states, which were suggested to be based on the two-quasiproton configuration [8,9], have lower energies. Since negative-parity proton pairs are excluded in our model space, in our calculation the first excited states with negative parity are taken as our negative-parity bands based on the 5_1^- and 6_1^- states, respectively. Similarly to the yrast band, in Fig. 1 one sees the irregular level energies for the 13_1^- state in the band based on the 5_1^- state and the 14_1^- state in the band based on the 6_1^- state given by Cal-1; in Fig. 2 one sees that the $B(E2, I \rightarrow I - 2)$ values of the band based on 5_1^- and the band based on 6_1^- given by Cal-1 drop significantly in the 13_1^- and 14_1^- states, respectively; and the g factors of these two bands decrease to negative values also in the 13_1^- and 14_1^- states. These features suggest that there are back-bending phenomena in the 13_1^- and 14_1^- states, given by the $(\nu h_{11/2})^{-2}$ alignment.

In Fig. 3(c), for the band based on the 5_1^- state, one sees that the subspace of SD pairs coupled to one negative-parity pair (i.e., Cal-5) presents a reasonable description of the states below the 13_1^- state (where the back-bending arises). For the 13_1^- state and the states above this state, the overlaps between the wave functions in Cal-1 and those in Cal-5 are close to 0, similarly to the case of the yrast band. In contrast, the overlaps between the wave functions in Cal-1 and those in Cal-3 are very close to 1, and the overlaps between the wave functions in Cal-3 and those in Cal-4 are also very large. This indicates that the $(\nu h_{11/2})^{-2}$ alignment in the 13_1^-, 15_1^-, and 17_1^- states can be essentially represented by the $H^{(10)}$ pair.

As for the band based on the 6_1^- state, one sees in Fig. 3(d) that the overlaps between the wave functions obtained in Cal-1 and those in Cal-3 are also close to 1. For each state, both the wave function in Cal-2 and that in Cal-4 well overlap with that

TABLE II. $B(E2)$ values (in W.u.) and g factors (in μ_N) for the yrast band and two negative-parity bands based on the 5_1^- and 6_1^- states. Theoretical results are obtained in the configuration space of Cal-1, and experimental data (expt) are taken from Ref. [27]. In this paper $e_\pi = 2e, e_\nu = -e$; $g_{\pi s} = 5.586 \times 0.7\mu_N, g_{\nu s} = -3.826 \times 0.7\mu_N$; and $g_{\pi l} = 0.90\mu_N, g_{\nu l} = 0.05\mu_N$.

| $J_i \to J_f$ | $B(E2)$ (W.u.) | | J^P | g factor (μ_N) | |
	Cal-1	Expt		Cal-1	Expt
$2_1^+ \to 0_1^+$	43.87	43(4)	2_1^+	0.331	0.34(3)
$4_1^+ \to 2_1^+$	59.45	–	4_1^+	0.323	–
$6_1^+ \to 4_1^+$	60.13	–	6_1^+	0.297	–
$8_1^+ \to 6_1^+$	30.56	–	8_1^+	0.038	–
$10_1^+ \to 8_1^+$	1.85	0.462(10)	10_1^+	−0.170	−0.159(5)
$12_1^+ \to 10_1^+$	11.78	–	12_1^+	−0.102	–
$14_1^+ \to 12_1^+$	47.78	–	14_1^+	−0.064	–
$16_1^+ \to 14_1^+$	43.65	–	16_1^+	0.014	–
$7_1^- \to 5_1^-$	3.49	–	5_1^-	−0.296	–
$9_1^- \to 7_1^-$	23.20	–	7_1^-	0.030	–
$11_1^- \to 9_1^-$	36.33	–	9_1^-	0.067	–
$13_1^- \to 11_1^-$	0.42	–	11_1^-	0.071	–
$15_1^- \to 13_1^-$	15.73	–	13_1^-	−0.110	–
$17_1^- \to 15_1^-$	13.58	–	15_1^-	−0.095	–
			17_1^-	−0.004	–
$8_1^- \to 6_1^-$	9.79	–	6_1^-	−0.010	–
$10_1^- \to 8_1^-$	32.46	–	8_1^-	0.052	–
$12_1^- \to 10_1^-$	50.89	–	10_1^-	0.062	–
$14_1^- \to 12_1^-$	0.17	–	12_1^-	0.072	–
$16_1^- \to 14_1^-$	3.88	–	14_1^-	−0.252	–
			16_1^-	−0.069	–

in Cal-3. As the spin increases, the overlaps between the wave functions in Cal-1 and those in Cal-5 decrease quickly, which means that the role of the $(\nu h_{11/2})^{-2}$ alignment becomes more

TABLE III. $B(E2)$ (in W.u.) and $B(M1)$ (in W.u.) calculated in the model space of Cal-1, for interband transitions between the band based on the 5_1^- state and the band based on the 6_1^- state.

| $J_i \to J_f$ | Cal-1 | |
	$B(E2)$	$B(M1)$
$6_1^- \to 5_1^-$	16.92	0.07
$7_1^- \to 6_1^-$	52.81	0.06
$8_1^- \to 7_1^-$	50.68	0.09
$9_1^- \to 8_1^-$	34.90	0.09
$10_1^- \to 9_1^-$	25.39	0.09
$11_1^- \to 10_1^-$	9.73	0.04
$12_1^- \to 11_1^-$	13.03	0.11
$13_1^- \to 12_1^-$	0.01	0.00
$14_1^- \to 13_1^-$	0.03	0.03
$15_1^- \to 14_1^-$	2.89	0.03
$16_1^- \to 15_1^-$	21.63	0.17
$17_1^- \to 16_1^-$	19.63	0.24

TABLE IV. Relative $B(E2)$ values for intraband transitions in the quasi-γ band and interband transitions from the quasi-γ band to the yrast band. Experimental values (expt) are taken from Ref. [13], and calculated results are obtained in the model space of Cal-1. For convenience we also present our calculated $B(E2)$ values of $2_2^+ \to 2_1^+$, $3_1^+ \to 2_2^+$, $4_2^+ \to 2_2^+$, $5_1^+ \to 3_1^+$, and $6_2^+ \to 4_2^+$; they are 25.2, 43.8, 34.6, 31.0, and 43.1 W.u., respectively.

$J_i \to J_f$	Cal-1	Expt
$2_2^+ \to 2_1^+$	100	100
$\to 0_1^+$	9.5	2.7(4)
$3_1^+ \to 2_2^+$	100	100
$\to 2_1^+$	4.1	2.6(4)
$\to 4_1^+$	19.6	38(6)
$4_2^+ \to 2_2^+$	100	100
$\to 3_1^+$	42.7	$\leqslant$50(11)
$\to 2_1^+$	1.3	1.8(3)
$\to 4_1^+$	38.2	73(10)
$5_1^+ \to 3_1^+$	100	100
$\to 4_2^+$	49.8	$\leqslant$45(7)
$\to 4_1^+$	1.8	$\leqslant$2.2(3)
$\to 6_1^+$	27.7	–
$6_2^+ \to 4_2^+$	100	–
$\to 5_1^+$	32.5	–
$\to 4_1^+$	0.1	–
$\to 6_1^+$	20.1	–

and more important; for the 14_1^- and 16_1^- states, the overlaps between the wave functions in Cal-1 and those in Cal-5 are close to 0, which means that the mechanism of the $(\nu h_{11/2})^{-2}$ alignment becomes dominant.

From the above discussion one sees common features of these four bands. Because the overlaps between the wave functions in Cal-1 and those in Cal-3 for the four bands are all close to 1 (with the exception of the 10_1^+ state, for which the overlap is about 0.8), the level spectra of Cal-3 are almost the same as the level spectra of Cal-1 in Fig. 1; and in Fig. 2, all $B(E2, I \to I - 2)$ values and g factors of Cal-3 are very close to those of Cal-1, except for $B(E2, 10_1^+ \to 8_1^+)$ and $B(E2, 12_1^+ \to 10_1^+)$. For the four bands in this paper, the overlaps between wave functions in Cal-2 and those in Cal-3 are close to the overlaps between Cal-1 and Cal-2, except for the 10_1^+ state in the yrast band. For the two negative-parity bands, the $(\nu h_{11/2})^{-2}$ alignment is reasonably represented by the coupling of two negative-parity pairs and better represented by the $H^{(10)}$ pair. The SD-pair approximation (with one additional negative-parity nucleon pair for the two negative-parity bands here) is able to present a reasonable description of both the yrast band and the band based on the 5_1^- state below the back-bendings, as well as the states of the quasi-γ band with lower spins.

IV. SUMMARY

In this paper we perform an NPA study of low-lying states in the ^{132}Ba nucleus. Our model space (denoted as Cal-1) is constructed of collective SD pairs for valence protons, coupled to the neutron valence space for which the building blocks

include SD pairs, all H pairs (consisting of two neutron holes in the $h_{11/2}$ orbit, with total spin 0, 2, 4, 6, 8, and 10), and the lowest-energy negative-parity pairs (with spin 4, 5, 6, and 7). This configuration space is the direct sum of that in Ref. [18] and that in Ref. [20] and is the largest model space of the NPA calculations for this nucleus hitherto. We show that, in addition to SD nucleon pairs, the H pairs and negative-parity nucleon pairs are complementary in describing the low-lying states of the ^{132}Ba nucleus.

In our calculation, the experimental level spectra, transition rates, and g factors are well reproduced. Our calculation shows that, in addition to the back-bending in the 10_1^+ state in the yrast band, back-bending phenomena arise in the 13_1^- state in the band based on the 5_1^- state and the 14_1^- state in the band based on the 6_1^- state, given by the $(\nu h_{11/2})^{-2}$ alignment.

We also perform the NPA calculations in relatively smaller spaces in comparison with Cal-1. By calculating the overlaps between wave functions in Cal-1 and those in a more restricted nucleon-pair space (Cal-2 to Cal-5), we are able to clarify the roles played by different nucleon-pair configurations. We show that the $(\nu h_{11/2})^{-2}$ alignment is reasonably represented by two negative-parity pairs and better represented by the spin-10 H pair. In order to well reproduce the experimental $B(E2, 10_1^+ \to 8_1^+)$, the configurations of negative-parity pairs are essential. The spin-8 H pair is important to the 8_1^+ state. The SD-pair approximation provides us with a good description of the yrast band before the back-bending and the states in the quasi-γ band with lower spins; coupled with one negative-parity neutron pair, the SD-pair approximation gives a reasonable description of the band based on the 5_1^- state below the back-bending; for the band based on the 6_1^- state, the simple description of SD coupled with one negative-parity pair deteriorates with spin and becomes almost irrelevant for states after the back-bending.

[1] G. Puddu, O. Scholten, and T. Otsuka, Nucl. Phys. A **348**, 109 (1980).

[2] R. F. Casten and P. Von Brentano, Phys. Lett. B **152**, 22 (1985).

[3] X. W. Pan, J. L. Ping, D. H. Feng, J. Q. Chen, C. L. Wu, and M. W. Guidry, Phys. Rev. C **53**, 715 (1996).

[4] Y. A. Luo and J. Q. Chen, Phys. Rev. C **58**, 589 (1998).

[5] Y. M. Zhao, S. Yamaji, N. Yoshinaga, and A. Arima, Phys. Rev. C **62**, 014315 (2000).

[6] L. Y. Jia, H. Zhang, and Y. M. Zhao, Phys. Rev. C **75**, 034307 (2007); **76**, 054305 (2007).

[7] A. Dewald, S. Harissopulos, G. Böhm, A. Gelberg, K. P. Schmittgen, R. Wirowski, K. O. Zell, and P. von Brentano, Phys. Rev. C **37**, 289 (1988).

[8] E. S. Paul, D. B. Fossan, Y. Liang, R. Ma, and N. Xu, Phys. Rev. C **40**, 1255 (1989).

[9] S. Juutinen, S. Törmänen, P. Ahonen, M. Carpenter, C. Fahlander, J. Gascon, R. Julin, A. Lampinen, T. Lönnroth, J. Nyberg, A. Pakkanen, M. Piiparinen, K. Schiffer, P. Šimeček, G. Sletten, and A. Virtanen, Phys. Rev. C **52**, 2946 (1995).

[10] S. Harissopulos, A. Gelberg, A. Dewald, M. Hass, L. Weissman, and C. Broude, Phys. Rev. C **52**, 1796 (1995).

[11] P. Das, R. G. Pillay, V. V. Krishnamurthy, S. N. Mishra, and S. H. Devare, Phys. Rev. C **53**, 1009 (1996).

[12] R. Kühn, K. Kirch, I. Wiedenhöver, O. Vogel, M. Wilhelm, U. Neuneyer, M. Luig, A. Gelberg, and P. von Brentano, Nucl. Phys. A **597**, 85 (1996).

[13] A. Gade, I. Wiedenhöver, H. Meise, A. Gelberg, and P. von Brentano, Nucl. Phys. A **697**, 75 (2002).

[14] S. Pascu, Gh. Căta-Danil, D. Bucurescu, N. Mărginean, C. Müller, N. V. Zamfir, G. Graw, A. Gollwitzer, D. Hofer, and B. D. Valnion, Phys. Rev. C **81**, 014304 (2010).

[15] A. Gelberg and A. Zemel, Phys. Rev. C **22**, 937 (1980).

[16] N. Yoshida, A. Arima, and T. Otsuka, Phys. Lett. B **114**, 86 (1982).

[17] H. Kusakari and M. Sugawara, Z. Phys. A **317**, 287 (1984).

[18] K. Higashiyama, N. Yoshinaga, and K. Tanabe, Phys. Rev. C **67**, 044305 (2003).

[19] T. Takahashi, N. Yoshinaga, and K. Higashiyama, Phys. Rev. C **71**, 014305 (2005).

[20] Y. Lei and Z. Y. Xu, Phys. Rev. C **92**, 014317 (2015).

[21] Y. Lei, G. J. Fu, and Y. M. Zhao, Phys. Rev. C **87**, 044331 (2013).

[22] J. Q. Chen, Nucl. Phys. A **626**, 686 (1997).

[23] Y. M. Zhao, N. Yoshinaga, S. Yamaji, J. Q. Chen, and A. Arima, Phys. Rev. C **62**, 014304 (2000).

[24] Y. M. Zhao and A. Arima, Phys. Rep. **545**, 1 (2014).

[25] G. J. Fu, Y. Lei, Y. M. Zhao, S. Pittel, and A. Arima, Phys. Rev. C **87**, 044310 (2013).

[26] I. Talmi, *Simple Models of Complex Nuclei* (Harwood Academic, Chur, Switzerland, 1993).

[27] http://www.nndc.bnl.gov/ensdf/.